Title	Arrott Plots and Magnetic Properties for Homogeneous and Heterogeneous Weakly Ferromagnetic Alloys
Author(s)	YAMADA, Hideji
Citation	[岐阜大学教養部研究報告] vol.[10] p.[163]-[176]
Issue Date	1974
Rights	
Version	岐阜大学教養部 (Department of Physics, Faculty of General Education, Gifu University)
URL	http://hdl.handle.net/20.500.12099/45996

Arrott Plots and Magnetic Properties for Homogeneous and Heterogeneous Weakly Ferromagnetic Alloys *

Hideji YAMADA

Department of Physics

(Received Sept. 30, 1974)

Abstract Using the Landau theory of phase transitions, Arrott plots for homogeneous and heterogeneous weakly ferromagnetic alloys are discussed. It is shown that Arrott plots for heterogeneous alloys deviate from the linear one. The influences of the spatial fluctuations in concentration on the magnetization, susceptibility and specific heat are discussed.

§ 1. Introduction

In 1968, Wohlfarth and his collaborators discussed the magnetic properties for weakly ferromagnetic metals and alloys.[1,2,3] Edwards and Wohlfarth [1] and Wohlfarth [2] discussed the dependences of temperature and magnetic field on the magnetization on the basis of the itinerant electron model and they got a good agreement between the theory and experiments for $ZrZn_2$. Mathon [3] discussed the magnetic behaviours of weakly ferromagnetic and strongly paramagnetic alloys, using the Landau theory of the phase transitions [4,5]. Mathon and Wohlfarth[6] applied this theory to Invar alloys (*f.c.c.* FeNi alloys about 30 at. % Ni) and got a good agreement with experiments. In these theory it is assumed that the magnetization is spatially homogeneous.

For the heterogeneous alloys, Wohlfarth [7] pointed that it should be possible in principle to gain information about the heterogeneities of the magnetization by comparing the results of experiments with theoretical predictions of the homogeneous alloys. On this point of view, Shtrikman and Wohlfarth [8] and Yamada and Wohlfarth [9,10] discussed the influences of fluctuations in concentration on the magnetic isotherms for weakly ferromagnetic alloys.

In § 2, we discuss the Arrott plots for the homogeneous alloys and in § 3

* This article is based on the lecture given by the author at the University of Lausanne, September, 1973.

for the heterogeneous alloys. In § 4, the influences of fluctuations in concentration on the susceptibility, magnetization and magnetic specific heat are discussed. In § 5, the present theory is compared with experiments.

§ 2. Homogeneous Weakly Ferromagnetic Alloys

Following the Mathon's paper[3], the free energy F of an alloy can be expanded in a power series in the magnetization as

$$F=\int f(\mathbf{r})\,d\mathbf{r}, \tag{1}$$

$$f(\mathbf{r})=f_0-M(\mathbf{r})H+\frac{1}{2}AM(\mathbf{r})^2+\frac{1}{4}BM(\mathbf{r})^4\left(+\frac{1}{6}CM(\mathbf{r})^6\right)+\frac{1}{2}D\,|\nabla M(\mathbf{r})|^2, \tag{2}$$

where $f(\mathbf{r})$ is the free energy density, f_0 its value for $M=0$ and $M(\mathbf{r})$ the magnetization density. A, B, C and D in (2) are expansion coefficients and depend on temperature and concentration. H is the magnetic field.

For weak ferromagnets, the higher order terms than M^6 can be neglected. On the other hand, the leading term of $f(\mathbf{r})$ due to the fluctuation of $M(\mathbf{r})$ is given by the last term in the right hand side of (2).[11] Higher order terms are given by $(\nabla M)^4$ and $(\nabla^2 M)^2$ but these terms are neglected if the fluctuation of $M(\mathbf{r})$ is small.[12]

Now minimizing (1) with respect to $M(\mathbf{r})$ gives

$$AM(\mathbf{r})+BM(\mathbf{r})^3+\left(CM(\mathbf{r})^5\right)-D\nabla^2 M(\mathbf{r})=H. \tag{3}$$

If $M(\mathbf{r})$ is homogeneous, (3) is reduced to the usual expression for weak itinerant ferromagnets given by Edwards and Wohlfarth[1] and Wohlfarth[2], that is,

$$F=\frac{1}{2}AM^2+\frac{1}{4}BM^4-MH, \tag{4}$$

and

$$AM+BM^3=H, \tag{5}$$

where

$$A=-\frac{1}{2\chi_0}\left\{1-\frac{T^2}{T_c^2}\right\}, \tag{6}$$

$$B=1/(2\chi_0 M_0^2), \tag{7}$$

χ_0 and M_0 are the high field susceptibilty and the magnetization at $T=0$ and $H=0$. T_c is the Curie temperature.

From (5), we get

$$\frac{H}{M}=A+BM^2, \tag{8}$$

which is shown in Fig. 1. The interceptions of lines with the horizontal axis give A and the gradients of lines give B^{-1}. When $H=0$, the lines for $A<0$

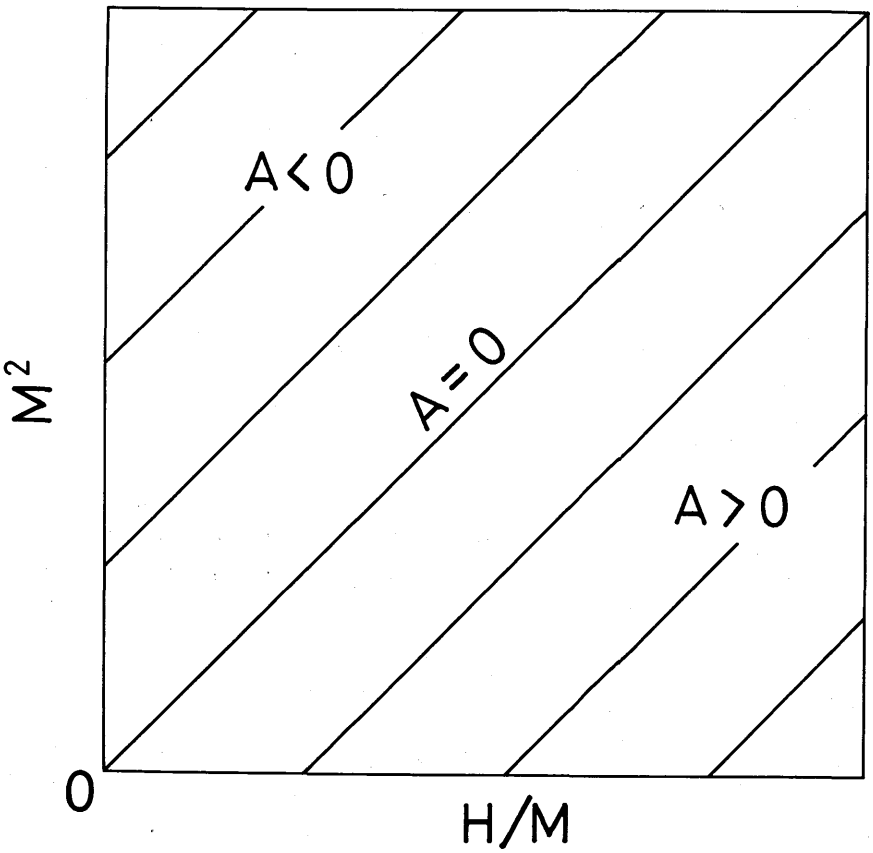

Fig. 1. Linear Arrott plots.

intercept with the vertical axis at finite positve values of M, but the lines for $A>0$ do not. Then $A<0$ means ferromagnetic state and $A>0$ means paramagnetic state. $A=0$ denotes the critical point between paramagnetic and ferromagnetic states, that is, the Curie temperature or critical concentration. Fig. 1 is well-known Arrott plots and it is very convenient to determine Curie temperature from these plots. It is easily obtained from (8) that the magnetization at $H=0$ and paramagnetic susceptibility χ are given by

$$M^2 = -\frac{A}{B}, \tag{9}$$

$$\chi = A^{-1}. \tag{10}$$

Next we discuss about the concentration dependence of A. Near the critical concentration c_0 between ferromagnetic and paramagnetic states, A is expanded in a power series of $|c-c_0|$ at $T=0$ as[3]

$$A(T=0) = a(c-c_0), \tag{11}$$

where the ferromagnetic state is for $c<c_0$ and the paramagnetic state for

$c > c_0$. From (9) and (11), we get

$$M(T=0)^2 = -\frac{a}{B}(c - c_0). \tag{12}$$

On the basis of the itinerant electron model, Edwards and Wohlfarth[1] and Wohlfarth[2] obtained

$$T_c \propto M(T=0), \tag{13}$$

then,

$$T_c^2 \propto c_0 - c. \tag{14}$$

From (6), (11) and (14), we can get

$$A(c, T) = a(c - c_0) + bT^2, \tag{15}$$

where b is a constant and a and b do not depend on c. Then the values specified by A in Fig. 1 (Arrott plots) mean the values of temperature or concentration. The arguments mentioned above are assumed that B is a positive constant. Next we discuss about the case of negative B.

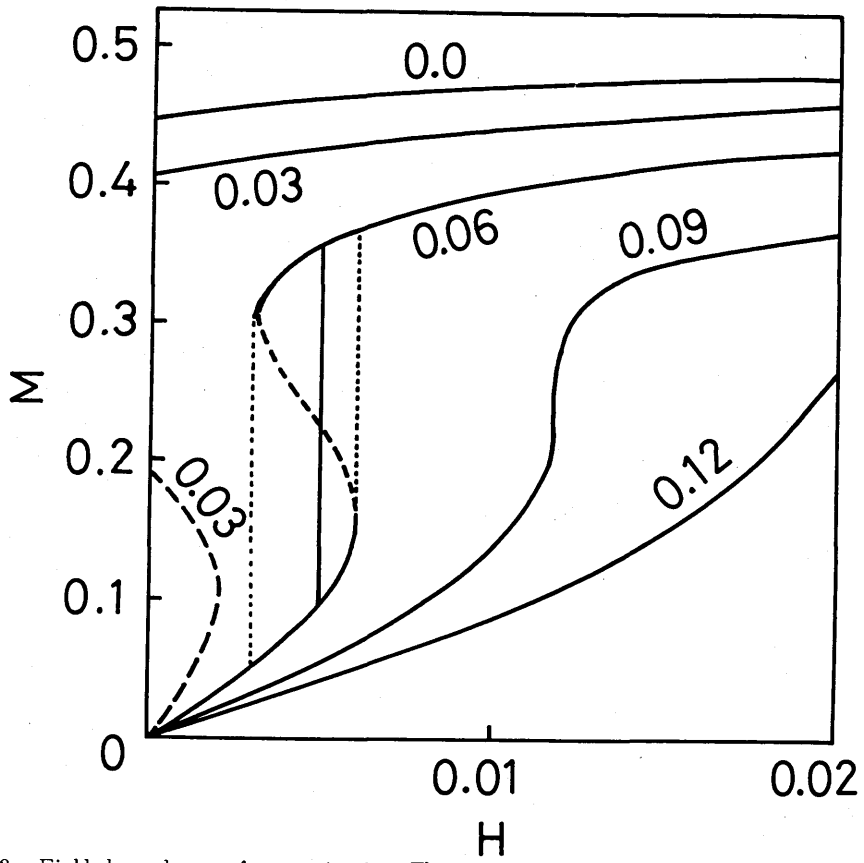

Fig. 2. Field dependence of magnetization. The numbers shown in the figure denote the values of A.

In the case of $B<0$, F in (4) decreases with increasing M because $B<0$. Then we must add $CM^6/6$ ($C>0$) to (4) in order to stabilize F at finite M, that is,

$$F=\frac{1}{2}AM^2+\frac{1}{4}BM^4+\frac{1}{6}CM^6-MH, \tag{16}$$

where $B<0$ and $C>0$. Minimizing (16) with respect to M gives

$$A+BM^2+CM^4=\frac{H}{M}. \tag{17}$$

Eq. (17) gives M as a function of H as shown in Fig. 2. In Fig. 2, calculated $M-H$ curves are shown for $B=-1$ and $C=5$. The numbers shown in the figure are the values of A. For $0<A<0.09$, M is a three-values function of H. Most stable solution in these three values of M is obtained by comparing the respective values of the free energy. In Fig. 3, the free energies for $A=0.06$ are shown

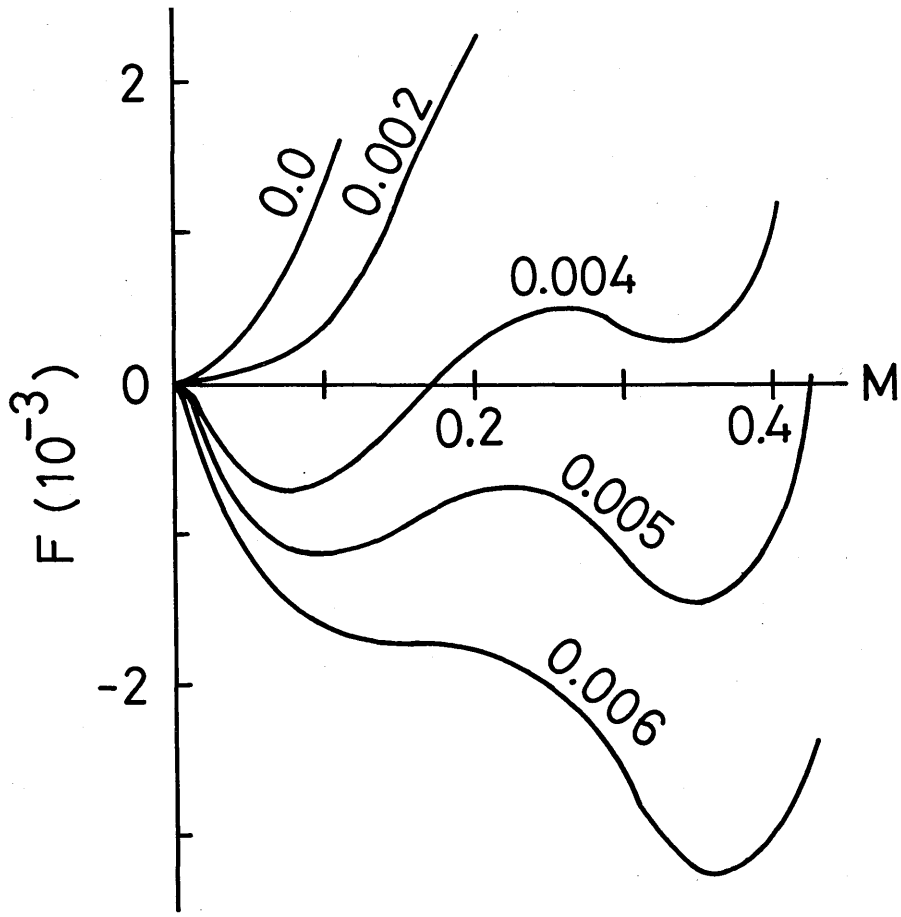

Fig. 3. Free energies for $A=0.06$ as a function of M for $H=0.0$, 0.002, 0.004, 0.005 and 0.006.

against M for various values of H. Three values of M correspond to two minimums and one maximum in the free energy and the state of lowest free energy is the stable solution. And M changes from the state of the small M to the state of the large M when H increases. This critical field is about 0.0049 in the case of Fig. 3. This is the collective electron metamagnetism discussed by Wohlfarth and Rhodes[13]. Shimizu[14] discussed such a first order transition in the ferromagnetic state.

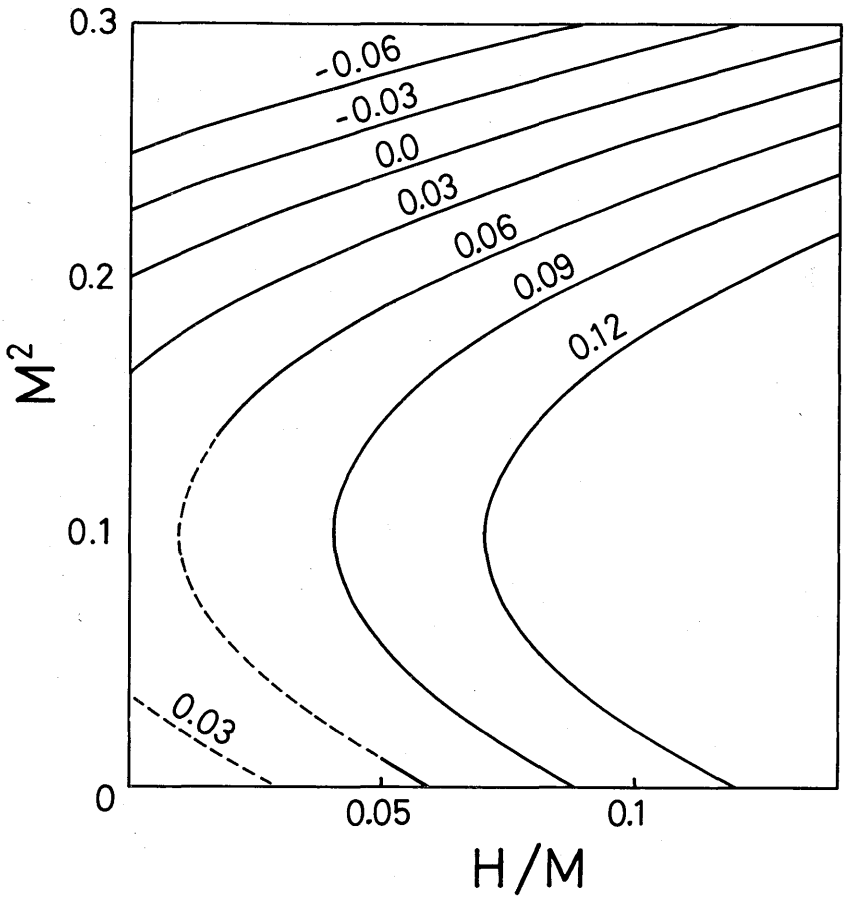

Fig. 4. Arrott plots. The numbers shown in the figure denote the values of A.

From (17), the Arrott plots are shown in Fig. 4. The numbers shown in the figure are the values of A and the broken curves in Fig. 4 are unstable states mentioned above.

§ 3. Heterogeneous Weakly Ferromagnetic Alloys[8,9]

In this section, we discuss the influence of heterogeneities on the results obtained in the previous section. The modification of the theory comes from;

(a) the dependence of the coefficients A, B and D in (2) on $\mathbf{r}$

(b) the gradient term in (2),

where we assume, for the simplicity, that $B>0$, so that we can neglect $CM^6/6$ in (2) for weak ferromagnets.

The dependence of A on $\mathbf{r}$ is given by (15) as

$$A(c(\mathbf{r}), T) = a(c(\mathbf{r}) - c_0) + bT^2. \tag{18}$$

Neglecting the dependences of B and D on $\mathbf{r}$, we get the following equation from (3) and (18),

$$A_0 M(\mathbf{r}) + BM(\mathbf{r})^3 - D\nabla^2 M(\mathbf{r}) + \{c(\mathbf{r}) - \langle c\rangle\} aM(\mathbf{r}) = H, \tag{19}$$

where

$$A_0 = a(\langle c\rangle - c_0) + bT^2, \tag{20}$$

and $\langle c\rangle$ means the average concentration defined by

$$\langle c\rangle = \frac{1}{V}\int d\mathbf{r}\, c(\mathbf{r}), \tag{21}$$

V is the volume of the specimen.

To calculate the average magnetization $\langle M\rangle$, we expand $M(r)$ and $c(r)$ into a Fourier series as

$$M(\mathbf{r}) = \langle M\rangle + \sum_k M_k \exp(i\mathbf{k}\cdot\mathbf{r}), \tag{22}$$

$$c(\mathbf{r}) = \langle c\rangle + \sum_k c_k \exp(i\mathbf{k}\cdot\mathbf{r}), \tag{23}$$

where

$$M_k^* = M_{-k} \quad \text{and} \quad c_k^* = c_{-k}. \tag{24}$$

Substituting (22) and (23) into (19), we get

$$A_0\{\langle M\rangle + \sum_k M_k \exp(i\mathbf{k}\cdot\mathbf{r})\} + B\{\langle M\rangle + \sum_k M_k \exp(i\mathbf{k}\cdot\mathbf{r})\}^3$$

$$+ D\sum_k k^2 M_k \exp(i\mathbf{k}\cdot\mathbf{r}) + a\sum_k c_k \exp(i\mathbf{k}\cdot\mathbf{r})$$

$$\times\{\langle M\rangle + \sum_k M_k \exp(i\mathbf{k}\cdot\mathbf{r})\} = H. \tag{25}$$

Assuming M_k and c_k are small, we get M_k in the first order term of c_k as

$$M_k = -\frac{a\langle M\rangle}{A_0 + 3B\langle M\rangle^2 + Dk^2} c_k. \tag{26}$$

Inserting (26) into (25) and integrating over $\mathbf{r}$, we obtain

$$A_0 + B\langle M\rangle^2 - \sum_k a^2 |c_k|^2 \frac{A_0 + Dk^2}{\{A_0 + 3B\langle M\rangle^2 + Dk^2\}^2}$$

$$= H/\langle M\rangle. \tag{27}$$

The last term on the left hand side of (27) can be expanded over the wave vector

k, assuming that the fluctuations in the concentration correspond to long wave lengths, and using the following relations

$$\sum_k |c_k|^2 = \langle \{c(\mathbf{r}) - \prec c \succ\}^2 \rangle,$$
$$\sum_k k^2 |c_k|^2 = \langle (\nabla c(\mathbf{r}))^2 \rangle, \tag{28}$$
$$\sum_k k^4 |c_k|^2 = \langle (\nabla^2 c(\mathbf{r}))^2 \rangle.$$

Neglecting higher order terms than $\langle (\nabla^2 c)^2 \rangle$, we can then obtain

$$x = A_0 - \frac{\alpha^2 A_0 + \beta^2}{(A_0 + 3y)^2} + \frac{2\beta^2 A_0}{(A_0 + 3y)^3} + y, \tag{29}$$

where

$$x = H/\langle M \rangle,$$
$$y = B\langle M \rangle^2,$$
$$\alpha^2 = a^2 \langle \{c(\mathbf{r}) - \prec c \succ\}^2 \rangle, \tag{30}$$
$$\beta^2 = a^2 D \langle (\nabla c)^2 \rangle.$$

We plot y against x (Arrott plots) for $\alpha^2 = 1.0$, $\beta^2 = 0.0$ in Fig. 5(a) and $\alpha^2 = 1.0$,

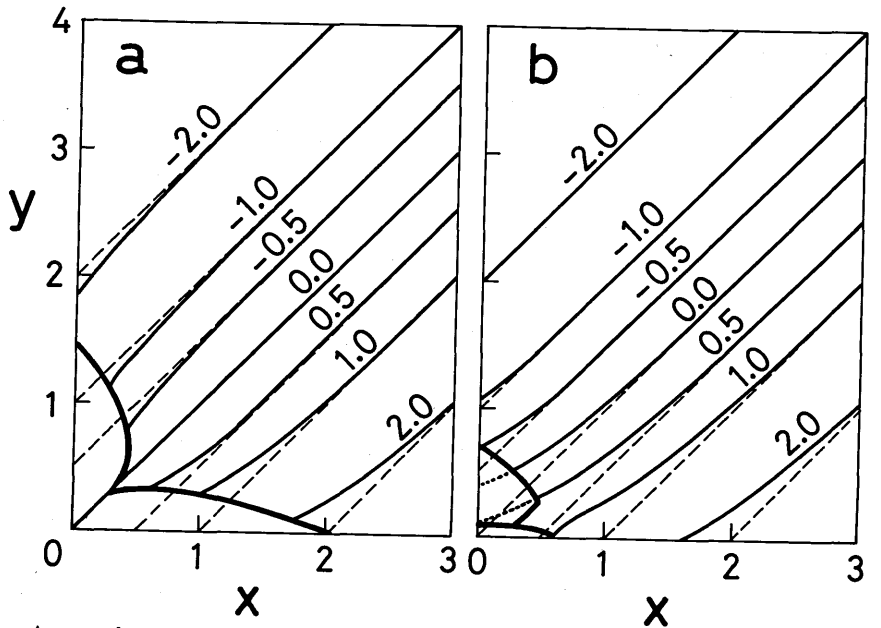

Fig. 5. Arrott plots for $\alpha^2 = 1.0$, $\beta^2 = 0.0$ in (a) and for $\alpha^2 = 1.0$, $\beta^2 = 0.6$ in (b). The numbers shown in figures denote the values of A_0.

$\beta^2 = 0.6$ in Fig. 5(b). Fig. 5(a) is the one obtained by Shtrikman and Wohlfarth[8]. The thick lines in Fig. 5 correspond to $dy/dx = 2$ and $1/2$. Inside these lines,

the present theory breaks down because the deviations of dy/dx from the usual linear Arrott plots ($dy/dx=1$) are too large. It is seen that the curves given by (29) deviate from the linear Arrott plots (broken lines in Fig. 5) in a characteristic way. At high values of x and y, the deviations are small, whereas nearer the origin they become large. The effect of β gives the following characteristic results:

(I) When $A_0 < -\beta^2/\alpha^2$ the curves tend to become more linear.

(II) When $0 > A_0 > -\beta^2/\alpha^2$ the curves bend upwards at smaller values of x rather than downwards.

(III) When $A_0 > 0$ the curves again tend to be rather more linear but continue to bend upwards.

These results are easily obtained by considering the signs of the second and third terms in (29). It is also concluded that the regions where theory breaks down become smaller if $\beta \neq 0$.

§ 4. Magnetic Properties

In this section, we discuss the influences of fluctuations in concentration on the susceptibility, magnetization and magnetic specific heat,

(a) *Susceptibility*[10]

Differentiation of (29) with respect to H gives the high field susceptibility which is easily shown to be given by

$$\chi_{hf} = \left\{ \frac{1}{2y}\left(\frac{dy}{dx}\right) \right\}_{x=0}, \tag{31}$$

that is to say, χ_{hf} is proportional to the ratio between the initial slope of the Arrott plots and $\langle M \rangle^2$ at $H=0$. From (29)

$$\left(\frac{dy}{dx}\right)_{x=0} = \left\{ 1 + 6\frac{\alpha^2 A_0 + \beta^2}{(A_0+3y)^3} - 18\frac{\beta^2 A_0}{(A_0+3y)^4} \right\}^{-1}. \tag{32}$$

The value of y in (31) and (32) is given by the solution of (29) for $x=0$. Calculated results of χ_{hf}^{-1} are shown in Fig. 6 for $\alpha^2=1.0$ and $\beta^2=0.0$, 0.1, 0,2, 0.3, 0.4, 0.5, 0.6 (the values of β^2 are shown in the figure). The broken line in Fig. 6 is that for the homogeneous case ($\alpha=\beta=0$), for which $\chi_{hf}^{-1} = -2A_0$. Note that for the large negative values of A_0 all curves of Fig. 6 have same slope, -2. The dotted curves in Fig. 6 are the values of χ_{hf}^{-1} in the region where the fluctuation of magnetization is big and the present theory breaks down. The calculated values of χ_{hf} for $\beta^2 \geqq 0.3$ show the presence of broad peaks near the Curie point or the critical concentration observed for Invar[15], NiCu[16], $ZrCu_{2-x}Al_x$[17] and PdNi alloys[18]. However, it is impossible to discuss the behaviour of χ_{hf} at the critical point because the fluctuation of magnetization becomes large there.

(b) *Magnetization*[9]

From (6), (7) and (29), we can obtain the following equation for the magnetization at $H=0$,

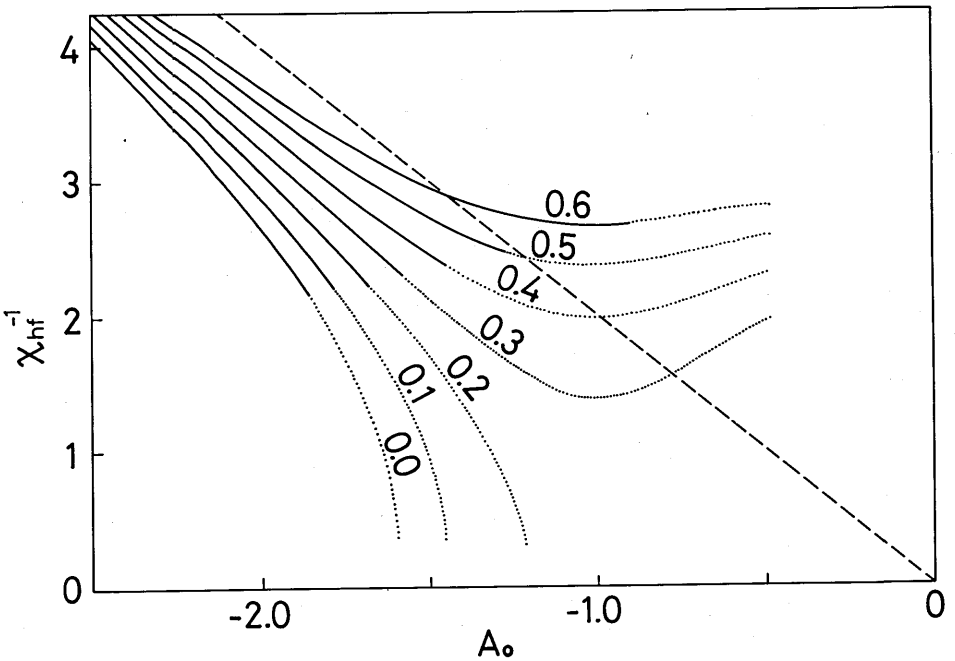

Fig. 6. The inverse high field susceptibility as a function of the Landau coefficient A_0. The numbers shown in the figure denote the values of β^2; $\alpha^2 = 1.0$.

$$\mu - \tau + \frac{\varepsilon_1{}^2 \tau - \varepsilon_2{}^2}{(3\mu - \tau)^2} - \frac{2\tau\varepsilon_2{}^2}{(3\mu - \tau)^3} = 0, \tag{33}$$

where

$$\left.\begin{aligned} \mu &= (\langle \mathrm{M} \rangle / \mathrm{M}_0)^2, \\ \tau &= 1 - (\mathrm{T}/\mathrm{T}_0)^2, \\ \varepsilon_1{}^2 &= 4\chi_0{}^2 \alpha^2, \\ \varepsilon_2{}^2 &= 8\chi_0{}^3 \beta^2, \end{aligned}\right\} \tag{34}$$

χ_0 and M_0 are the high field susceptibility and the magnetization at $T=0$, and T_0 is the Curie temperature for the homogeneous case ($\alpha=\beta=0$). Fig. 7 shows the temperature dependence of $\langle M \rangle$ for $\varepsilon_1{}^2 = 0.16$, $\varepsilon_2{}^2 / \varepsilon_1{}^2 = 0.0$, 0.1, 0.2 and 0.3. The broken curve in Fig. 7 is that for the homogeneous case ($\varepsilon_1 = \varepsilon_2 = 0$). The value of $\langle M \rangle$ in the regions where theory breaks down is shown by dotted curves. Fig. 7 shows higher Curie temperature T_c than the homogeneous one T_0. The curve specified by $A_0 = 0$ ($T = T_0$) in Fig. 5(b) bends upwards and crosses the y-axis at a finite positive value, corresponding to ferromagnetism, so that $T_c > T_0$. This result has the following physical meaning: The gradient term in the free energy in (2) makes M smooth by decreasing it where it was previously large and increasing it where it was previously small. But corresponding free energy gained is proportional to $|A| \Delta^2$, where Δ is the change of M. This gain

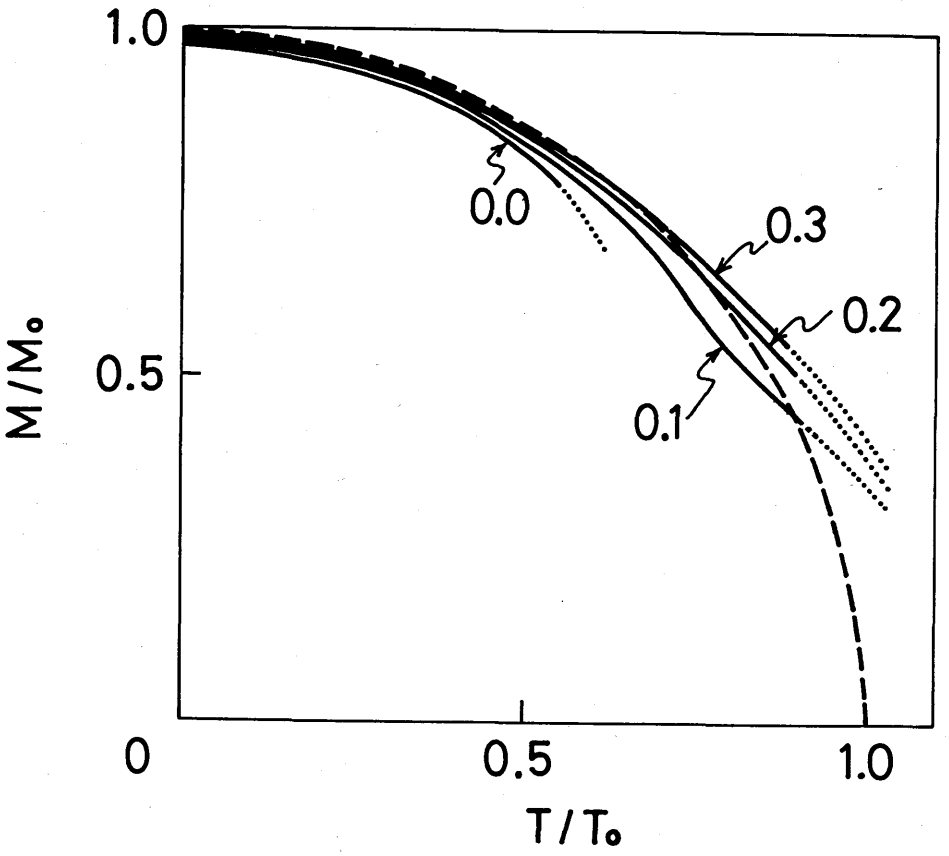

Fig. 7. Temperature dependence of the magnetization for $\varepsilon_1^2 = 0.16$, $\varepsilon_2^2/\varepsilon_1^2 = 0.0$, 0.1, 0.2 and 0.3.

is less if the decrease Δ is small, i.e., the magnetization remains large, in the more strongly ferromagnetic regions of large $|A|$ and there is a relatively larger increase of M in the less strongly ferromagnetic regions of small $|A|$. The effect is thus a general increase of M and T_c. Unfortunately, the Curie temperature T_c cannot be obtained because T_c lies inside the regions where the theory breaks down. But if we plot $\langle M \rangle / M_0$ against T/T_c, the curves will infact drop more sharply at lower temperatures and tend to zero at $T/T_c = 1$. Predicted trend is in good agreement with experiments[19].

(c) *Magnetic Specific Heat*

The magnetic part of the free energy (1) at $H=0$ is given by

$$\frac{\Delta F}{M_0^2} = -\frac{1}{4\chi_0}\tau\mu + \frac{1}{8\chi_0}\mu^2 - \frac{\varepsilon_1^2}{4\chi_0(3\mu-\tau)} + \frac{\varepsilon_2^2}{4\chi_0(3\mu-\tau)^2} \tag{35}$$

Then the magnetic part of the specific heat is given by

$$\Delta C = -T\frac{d^2\Delta F}{dT^2}$$

$$= -\frac{M_0{}^2 T}{2\chi_0 T_0{}^2}\left[\mu\left\{1+\frac{\varepsilon_1{}^2}{(3\mu-\tau)^2}-2\frac{2\varepsilon_1{}^2(1-\tau)+\varepsilon_2{}^2}{(3\mu-\tau)^3}+12\frac{\varepsilon_2{}^2(1-\tau)}{(3\mu-\tau)^4}\right\}\right.$$

$$\left.+T\frac{d\mu}{dT}\left\{1+\frac{\varepsilon_1{}^2}{(3\mu-\tau)^2}-2\frac{3\varepsilon_1{}^2\mu+\varepsilon_2{}^2}{(3\mu-\tau)^3}+18\frac{\varepsilon_2{}^2\mu}{(3\mu-\tau)^4}\right\}\right], \qquad (36)$$

where

$$\frac{d\mu}{dT} = -\frac{\chi_{hf} T\langle M\rangle}{\chi_0 T_0{}^2 M_0}\left\{1-\frac{\varepsilon_1{}^2}{(3\mu-\tau)^2}-2\frac{\varepsilon_1{}^2\tau-2\varepsilon_2{}^2}{(3\mu-\tau)^3}+6\frac{\varepsilon_2{}^2\tau}{(3\mu-\tau)^4}\right\}. \qquad (37)$$

The calculated results of ΔC for $\varepsilon_1{}^2 = 0.16$ and $\varepsilon_2{}^2/\varepsilon_1{}^2 = 0.0$, 0.1, 0.2, 0.3 are shown in Fig. 8. The numbers in the figure denote the values of $\varepsilon_2{}^2/\varepsilon_1{}^2$. The

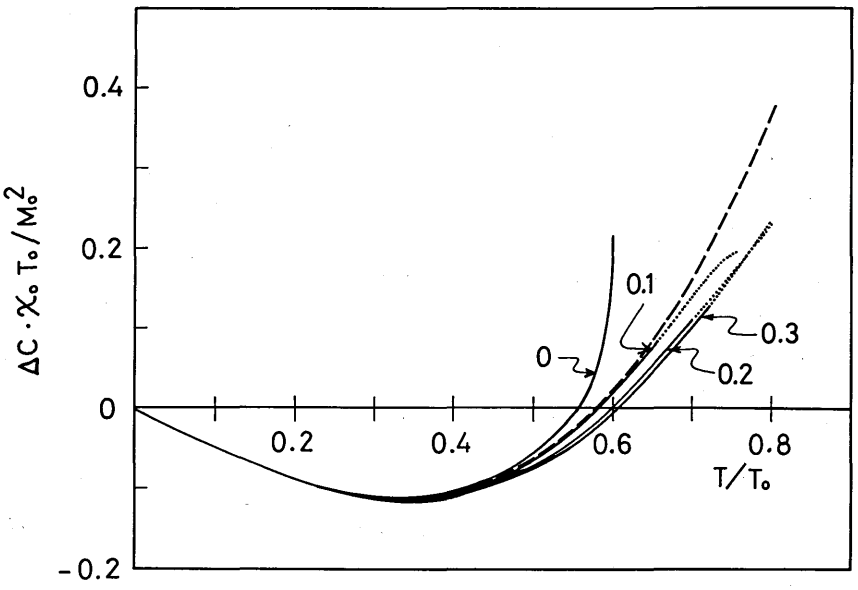

Fig. 8. Temperature dependence of the magnetic specific heat for $\varepsilon_1{}^2 = 0.16$, $\varepsilon_2{}^2/\varepsilon_1{}^2 = 0.0$, 0.1, 0.2 and 0.3.

broken curve in Fig. 8 is that for the homogeneous case ($\varepsilon_1 = \varepsilon_2 = 0$). The values of ΔC in the regions where the theory breaks down are shown by dotted curves. As for χ_{hf}, the behaviour near the critical point cannot be discussed. However it appears that the specific heat deviates less from the homogeneous result than is the case for χ_{hf}, but that the magnetic entropy differs significantly for a heterogeneous as compared to a homogeneous alloy.

§ 5. Summary of Experimental Data and Discussion

In § 2 and § 3, we discussed the Arrott plots for homogeneous and

heterogeneous weakly ferromagnetic alloys. In this section, we summarize a lot of experimental data and compare them with the results obtained in this paper.

(a) $Zr_{1-x}M_xZn_2$ ($M=Ti$, Hf)[20,21], Ni_3Al[22,23], Ni_3Ga[22,23], Invar[15,24], NiPt alloys[25]

These materials show the linear Arrott plots as shown in Fig. 1. The small deviations from the linear Arrott plots could be explained by the heterogeneities discussed in § 3. However, it is not clear that the anomalies in the small M region for Ni_3Ga[23] can be explained by the heterogeneities.

(b) PdNi alloys[26,27]

Below 3 at.% Ni, the shape of Arrott plots is similar to Fig. 5(b) at any temperature. Between 3 and 5 at.% Ni, Arrott plots exhibit like Fig. 5(a). Above 5 at.% Ni, linear Arrott plots are obtained.

(c) Sc_3In[28,29], NiCu alloys[16,30]

These materials do not show linear Arrott plots. These plots bend downwards. Our result of Fig. 5(b) has opposite tendency. In our theory of § 3, it is assumed that the fluctuations in the concentrations are small, so that we may not be able to apply the present theory to the materials with clusters (*e.g.*, NiCu alloys).

In this paper, we discussed the Arrott plots for homogeneous and heterogeneous weakly ferromagnetic alloys and the influences of the heterogeneities on the magnetic properties, using the Landau theory of phase transitions and assuming that the fluctuations in the concentrations are small. Another approach for discussing the influence of the heterogeneity on the magnetic property has been done by Edwards *et al*[31]. They obtained the dependence of M on the position based on (3) and applied their theory to the paramagnetic PdNi alloys.

References

1) D. M. Edwards and E. P. Wohlfarth: Proc. Roy. Soc., **303** 127, (1968).
2) E. P. Wohlfarth; J. Appl. Phys., **39** 1061, (1968).
3) J. Mathon: Proc. Roy. Soc., **306** 355, (1968).
4) L. Landau and E. M. Lifshitz: *Statistical Physics* (London, Pergamon) (1958).
5) L. P. Kadanoff, W. Götze, D. Hamblen, R. Hecht, E. A. S. Lewis, V. V. Palciauskas, M. Rayl, J. Swift, D. Aspnes and J. Kane: Rev. Mod. Phys., **39** 395, (1967).
6) J. Mathon and E. P. Wohlfarth: Phys. Stat. Sol., **30** Kl31, (1968).
7) E. P. Wohlfarth: J. Phys., **32** Cl-636, (1971).
8) S. Shtrikman and E. P. Wohlfarth: Physica, **60** 427, (1972).
9) H. Yamada and E. P. Wohlfarth: Phys. Stat. Sol. (b), **58** Kl51, (1973).
10) H. Yamada and E. P. Wohlfarth: Phys. Stat. Sol. (b), **64** K74, (1974).
11) C. Herring and C. Kittel: Phys. Rev., **81** 869, (1951).
12) M. Shimizu and H. Yamada: J. Phys. Soc. Japan, **21** 621, (1966).
13) E. P. Wohlfarth and P. Rhodes: Phil. Mag., **8** 1817, (1962).
14) M. Shimizu: Proc. Phys. Soc., **84** 397, (1964), *ibid* **86** 147, (1965).
15) O. Yamada, R. Pauthenet and J. C. Picoche: J. Phys., **32** Cl-1119, (1971).

16) F. Acker and R. Huguenin: Phys. Letters, **28** 343, (1972).
17) G. S. Knapp, F. Y. Fradin and H. V. Culbert: J. Appl. Phys., **42** 1341, (1971).
18) G. Chouteau, R. Fourneaux, K. Gobrecht and R. Tournier: Phys. Rev. Letters, **20** 193, (1968).
19) P. Mazzetti, G. Montalenti and G. P. Soardo: J. Phys., **33** 113, (1972).
20) S. Ogawa and N. Sakamoto: J. Phys. Soc. Japan, **22** 1214, (1967).
21) S. Ogawa: J. Phys. Soc. Japan, **25** 109, (1968).
22) F. R. deBoer, C. J. Schinkel, J. Biesterbos and S. Proost: J. Appl. Phys., **40** 1049, (1969).
23) C. J. Schinkel, F. R. de Boer and B. de Hon: J. Phys. F, **3** 1463, (1973).
24) G. F. Bolling, A. Arrott and R. H. Richman: Phys. Stat. Sol., **26** 743, (1968).
25) J. Beille. D. Bloch and E. P. Wohlfarth: Phys. Letters, **43** A 207, (1973).
26) J. Beille, D. Bloch and M. J. Besnus: J. Phys. F, **4** (1974) *to be published.*
27) J. Beille: *preprint.*
28) W. E. Gardner, T. F. Smith, B. W. Howlett, C. W. Chu and A. Sweedler: Phys. Rev., **166** 577, (1968).
29) E. Fawcett and P. P. M. Meincke: J. Phys., **32** Cl-629, (1971).
30) C. G. Robbins, H. Claus and A. Beck: J. Appl. Phys., **40** 2269, (1969).
31) D. M. Edwards, J. Mathon and E. P. Wohlfarth: J. Phys. F, **3** 161, (1973).